A Systematic Design Method of On-Glass Antennas Using Mesh-Grid Structures

Seungbeom Ahn, *Student Member, IEEE*, and Hosung Choo, *Member, IEEE*

***Abstract*—In this paper, we propose a systematic design method for an on-glass antenna, which is suitable for receiving frequency modulation (FM) radio in a commercial recreational vehicle (RV). For the main antenna body, we used a mesh-grid structure that most efficiently uses the given space of the glass for broad-matching bandwidth. To obtain the detail design parameters that exhibit optimum radiating performance, we used a genetic algorithm (GA) in conjunction with a full-wave electromagnetic (EM) simulator. To reduce the searching space in our GA process, we applied a connection-warranted filtering. After the GA optimization, we also applied a shape-simplification process and a transparency-improvement process to broaden the passenger's field of view. The designed antenna shows an average gain of about -9.05 dBi along the bore-sight direction ($\theta = 90^\circ, \phi = 270^\circ$) in the FM radio band (80–120 MHz), which is 10 dB higher than a commercial roof-mounted microantenna. Finally, the operating principle of the proposed antenna was examined by using a lumped-element circuit model, and these results confirmed that the proposed antenna is well suited for FM radio reception in commercial RVs.**

***Index Terms*—Mesh-grid structure, on-glass antenna, vehicle antenna.**

I. Introduction

AMPLITUDE modulation (AM)/frequency modulation (FM) radio is one of the most widely used communication systems in a wide range of vehicles types [1]. The receiving performance of AM/FM radio is usually considered as a primary factor that affects vehicle evaluation by ordinary customers. Thus, most of vehicle manufacturers spend substantial effort in improving their radio systems and offer their own performance standard in AM/FM reception. The AM/FM radio consists of a tuner, an amplifier, a connection cable, and a receiving antenna. Of these, the receiving antenna, in particular, is the most important device, having a critical effect on the reception performance.

Generally, monopole-type antennas, such as the conventional $\lambda/4$ monopole, tuned monopole, roof-mounted microantenna, and shark-fin-shaped antenna, have widely been used for AM/FM receiving antennas in various types of vehicles [2]–[4]. However, both antennas suffer from lack of durability and the undesirable appearance of protruding from the vehicles. To mitigate these problems, on-glass antennas directly printed on the rear or quarter glasses of a vehicle have been developed and are now commonly applied in many commercial vehicles [5]–[8]. This on-glass antenna can drastically reduce a manufacturing cost since the antenna's conducting body is printed on the window, using a cheaper silk-screening printing method. In addition, multiple antennas that operate for various applications or different frequency bands can easily be packed in a single window.

The on-glass antenna, however, provides relatively low vertical gain and narrow bandwidth, compared with a monopole-type antenna, because the strip of the antenna body is printed on the glass with high dielectric loss. The on-glass antenna may also exhibit nulls in its radiation patterns, because it is placed in close proximity to the conducting frame of the vehicle. Furthermore, there are some restrictions in the on-glass antenna design, because the antenna should not block the passenger's field of view.

In this paper, we propose a systematic design method for the on-glass antenna that makes it suitable for use in FM radio reception of a commercial recreational vehicle (RV). For the main frame of the antenna body, we used a mesh-grid structure that most efficiently uses the given space of the quarter glass to broaden the operating bandwidth and increase the antenna's radiation efficiency [6]. In the design procedure, we first optimized the antenna structure by using a genetic algorithm (GA), in conjunction with an electromagnetic (EM) simulator. For accurate estimation of antenna performance, the entire vehicular structure, as well as the antenna body, was inserted into the EM simulation. To reduce the searching space and the total optimization time, we applied a connection-warranted filtering (CWF) that removes strips that are disconnected from the feeder. In addition, we used the shape-simplification process (SSP) and transparency-improvement process (TIP), which can broaden the passenger's field of view. The finalized antenna design was built and mounted on a commercial RV, and the antenna characteristics, such as the matching bandwidth and bore-sight gain, were measured in a semianechoic chamber. Then, the operating principle of the proposed antenna was analyzed using the lumped element circuit model and current distributions flowing through strips.

This paper is organized as follows: Section II presents the geometry of the proposed mesh-grid antenna structure and the method of optimization. Section III describes the measurement results and the operating principles of the antenna, and Section IV presents the conclusions.

Manuscript received September 6, 2009; revised April 9, 2010; accepted May 17, 2010. Date of publication June 17, 2010; date of current version September 17, 2010. This work was supported in part by Hyundai·Kia Motors and in part by the IT R&D program of MKE/KEIT (KI002084, A Study on Mobile Communication Systems for Next-Generation Vehicles with Internal Antenna Array). The review of this paper was coordinated by Prof. S. K. Chaudhuri.

The authors are with the School of Electronic and Electrical Engineering, Hongik University, Seoul 121-791, Korea (e-mail: sa015366@hongik.ac.kr; hschoo@hongik.ac.kr).

Color versions of one or more of the figures in this paper are available online at http://ieeexplore.ieee.org.

Digital Object Identifier 10.1109/TVT.2010.2053227

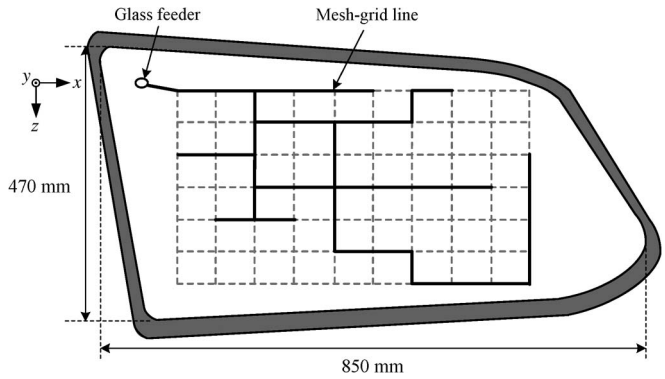

Fig. 1. Mesh-grid structure.

II. Antenna Structure and Optimization

A. Antenna Optimization

Due to ignition noise from an engine and a wiper, the front glass is not usually used for on-glass antennas. Therefore, RVs generally use a quarter glass, which is placed on the rear left of the vehicle body, as a printed on-glass antenna. The antenna's main body consists of conducting strips directly printed on the glass surface by using a silk-screening printing method. The size of the antenna should be miniaturized in order for the strips to be filled in the small quarter window. Various design structures can be used as the on-glass antenna for these RVs. For example, a simple straight strip or a bent strip is commonly used as the basic design structure for many RVs. However, these structures usually exhibit low-matching bandwidths and radiation gains.

To improve the antenna performance over conventional designs, we employ a mesh-grid structure as an antenna body. The mesh-grid shape intrinsically has a structural advantage of achieving a broad-matching bandwidth, because it can more efficiently use the given antenna space by more uniformly and widely distributing the currents. Fig. 1 shows the antenna design using the mesh-grid structure. The mesh grid is placed on the glass window, which has dielectric material properties of $\varepsilon_{\rm r} = 7$ and tan $\delta = 0.03$ at 100 MHz. The size of the quarter glass is 850 mm $\times$ 470 mm, and the design space of 720 mm $\times$ 390 mm in the quarter glass is used as the whole mesh grid. Thus, each grid cell has the dimension of 80 mm $\times$ 65 mm. In each grid cell, the conducting strip only resides along the solid string, and there is no conducting strip along the dashed string. Therefore, the currents flow through the conducting strips, which are linked with the feeder that is placed on the upper left of the mesh grid.

To estimate the antenna performance, such as reflection coefficient or radiation gain, we used FEKO from EM Software and Systems [9]. For accurate performance estimation, the whole vehicle body should be considered in the EM simulation since the size of the vehicle is about 2 λ in the FM band. Therefore, the entire commercial RV (2006 KIA Grand Carnival) is modeled as a 3300-piecewise mesh, as shown in Fig. 2(a). As shown in Fig. 2(b), the antenna is fed by a coaxial cable $(Z_0 = 50\ \Omega)$ from the upper left corner of the quarter glass. The feeder to the on-glass antenna is connected with the vehicle frame through a low-noise amplifier (LNA), but, in the

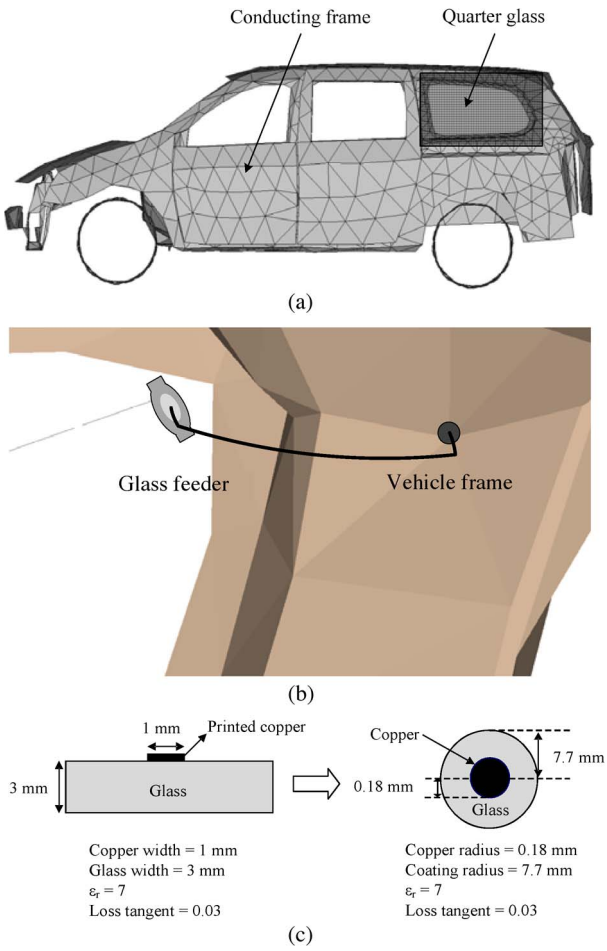

Fig. 2. Simulation condition. (a) Vehicular structure. (b) Feeding structure. (c) Coated-wire method.

simulation, the feeding line is directly connected to the vehicle frame without the LNA. For faster EM simulation, the strips printed on a quarter glass window are approximately modeled as coated wire, which assumes that the inner conducting wire is coated by dielectric materials, as shown in Fig. 2(c). For a 1-mm-width (150-μm-thick) copper strip printed on 3-mm-thick glass, the equivalent radius is modeled as a 0.25-mm copper wire surrounded by a 9-mm-radius dielectric $(\varepsilon_r = 7)$ coating [10], [11]. We then experimentally detuned the radius by comparing the simulations and the measurements and found the copper radius of 0.18 mm and the coated radius of 7.7 mm.

To obtain the optimum mesh-grid design that achieves the broad-matching bandwidth and high radiation gain, we used a GA in conjunction with the EM simulation [12]–[14]. In our GA, the mesh-grid structures are encoded as binary chromosomes consisting of 2-D binary arrays. Basically, chromosomes are made of 123 (vertical segments: 6 $\times$ 10, horizontal segments: 9 $\times$ 7) binary bits, where the "0" bit means "no conducting strip," and the "1" bit means "conducting strip." We choose the size (80 mm $\times$ 65 mm) of the cell to finish the optimization process (ten iterations) within one day, considering our computational resource (Quad CPU with 2.40 GHz). Thus, each chromosome represents a single mesh-grid design, and the chromosomes evolve to have improved antenna performances during the GA iteration. However, the disadvantage of the

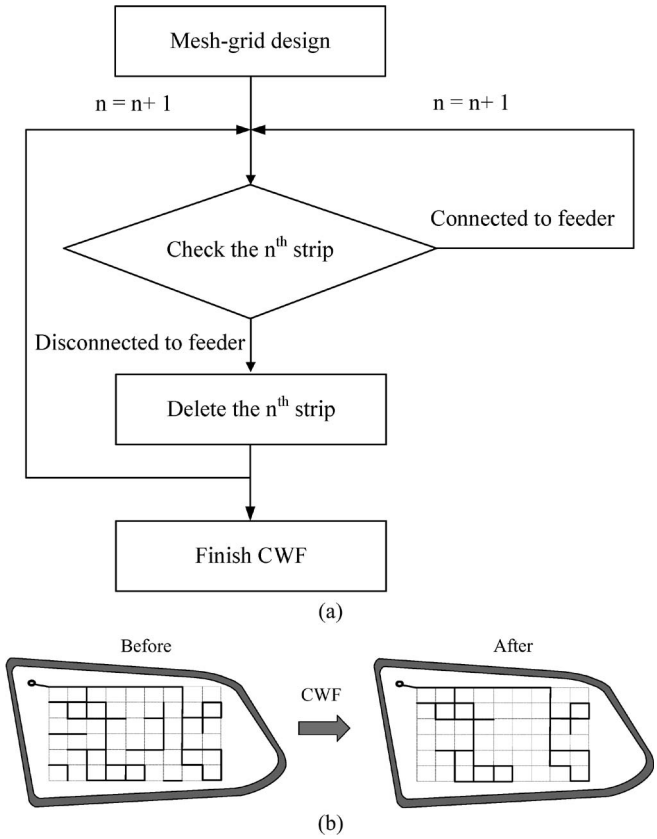

Fig. 3. Connection warranted filtering. (a) Diagram. (b) Example of CWF.

mesh-grid structure is the relatively long optimization process time, because the mesh-grid design has too many design freedoms that produce a large searching space of $2^{6\times10} \times 2^{9\times7}$. To efficiently reduce the searching space with minimum loss of antenna performance, we use CWF [see Fig. 3(a)]. As can be seen in the figure, CWF filters out the strips that are not connected to a feeder. Using CWF, we can simplify the antenna design without much loss of antenna performance, because stronger currents generally flow through strips directly connected by a feeder, compared with isolated strips. An example of CWF is shown in Fig. 3(b). After CWF filtering, some disconnected strips are filtered out, and as a result, 11 strip segments are deleted.

To more effectively receive FM radio signals, the receiving antenna should have higher vertical gain along the bore-sight direction $(\theta = 90^\circ, \phi = 270^\circ)$. To achieve this design goal, we define a fitness function in our GA process as follows:

$$fitness = \frac{1}{N}\sum_{i=1}^{N}\left[Gain\left\{f_i(\theta = 90^\circ, \phi = 270^\circ)\right.\right. \\ \left.\left. f_i = 80 \sim 120\ \text{MHz}\right\}\right]. \quad (1)$$

The fitness function represents average gain along the bore-sight direction $(\theta = 90^\circ, \phi = 270^\circ)$ in the FM radio band (80–120 MHz). Then, GA continuously searches the designs with higher fitness values during the GA process. Fig. 4 shows the fitness value in terms of GA iterations. The fitness value is increased up to 0.14, which represents -8.39-dBi average vertical gain after about 40 GA iterations.

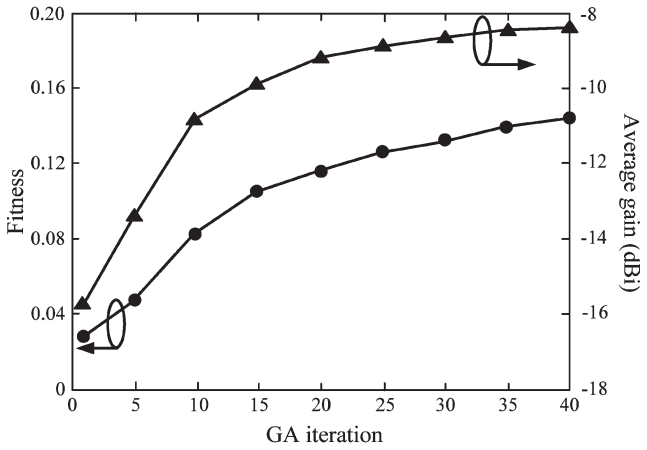

Fig. 4. GA optimized results.

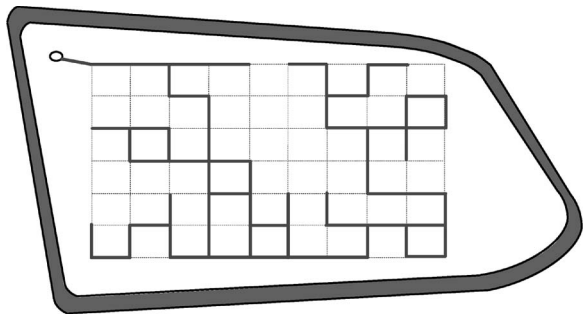

Fig. 5. Optimized on-glass antenna.

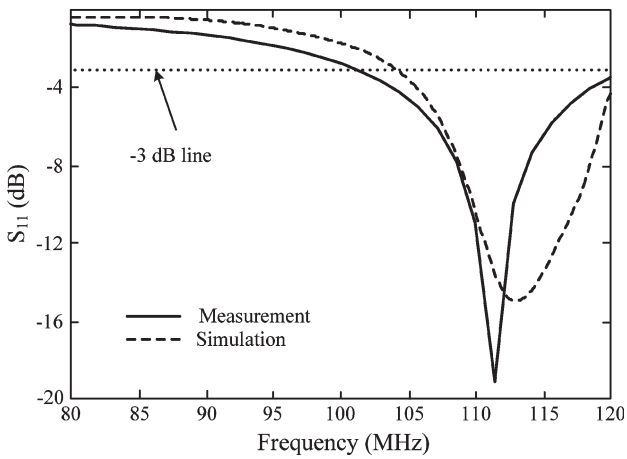

Fig. 6. Reflection coefficient of the optimized on-glass antenna.

Fig. 5 shows the optimized antenna, which shows the U-type structure. To verify the optimized antenna's performance, an on-glass antenna with 1-mm strip width was built, and the measurement was performed using an Agilent E5071A network analyzer with an ETS-Lindgren 3121C dipole as the transmitter [15]. Fig. 6 shows the (solid line) measured and (dashed line) simulated reflection coefficient of the optimized antenna. The measured result is similar to the simulation, and it shows a 3-dB bandwidth of around 20% (102–122 MHz). Although the reflection coefficient is relatively high from 80 to 90 MHz, the bore-sight gain of the optimized antenna is more than -20 dBi in the entire FM radio band.

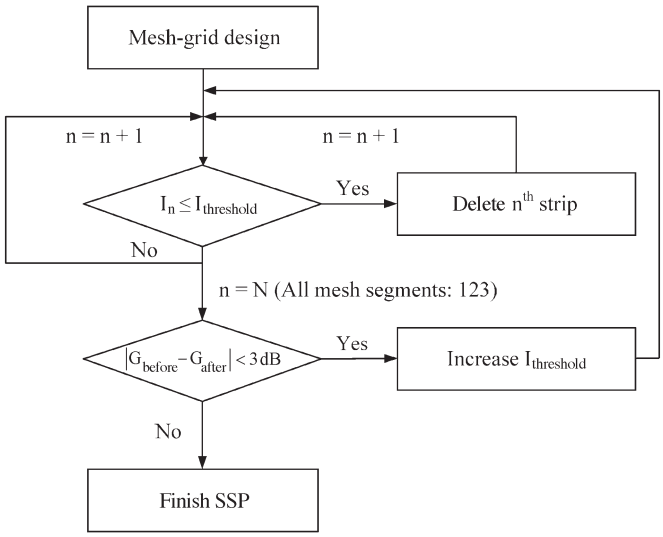

Fig. 7. Diagram of SSP.

B. Design Modification for the Mass Production

The shape of the on-glass antenna should visually be simple and have high optical transparency, because the on-glass antenna should minimize obstruction of the passenger's view. However, the optimized design has a somewhat complicated structure, which occupies about 50% of the total mesh grid. Therefore, to improve the appearance of our on-glass antenna, we applied further design steps of the SSP and TIP.

Fig. 7 shows a block diagram of the SSP. The procedure starts from examining the current distribution on each strip segment. If the amplitude of the current is lower than a certain reference value $(I_{\mathrm{threshold}})$, then the strip segment is removed from the design. The bore-sight gain of the design before and after the SSP is then compared to see the variation in antenna performance. This procedure is repeated until the gain variation is more than 3 dB, compared with that of the original design. Using SSP, we can simplify the design by removing the strip that may not have a critical effect on antenna performance. Fig. 8 shows a simplified design after the first, second, and third iterations of SSP. At the first, second, and third iterations, strip segments with the current amplitude (space averaged) lower than -50, -45, and -40 dBA, respectively, are removed (see Fig. 8). Fig. 9(a) shows the simulated bore-sight gains. The antennas after the first and second iterations have similar bore-sight gains in which the variation is less than 1 dB. However, the antenna after the third iteration shows a significantly lower bore-sight gain of less than 3 dB, compared with the original design. Fig. 9(b) shows the average current distributions on the strips of the antenna. As the number of iterations increases, the average current on the strip also increases. Table I presents detailed comparisons of the antenna performance after SSP, where the occupancy rate is indicated by the ratio of the used strips to the total mesh grid. Using this SSP method, we can decrease the occupancy rate from 50% to 31%, whereas the bore-sight gain maintains similar results to the original design, differing by only 1 dB.

To better improve the field of view of the quarter window, we applied the TIP on the on-glass antenna design. A block

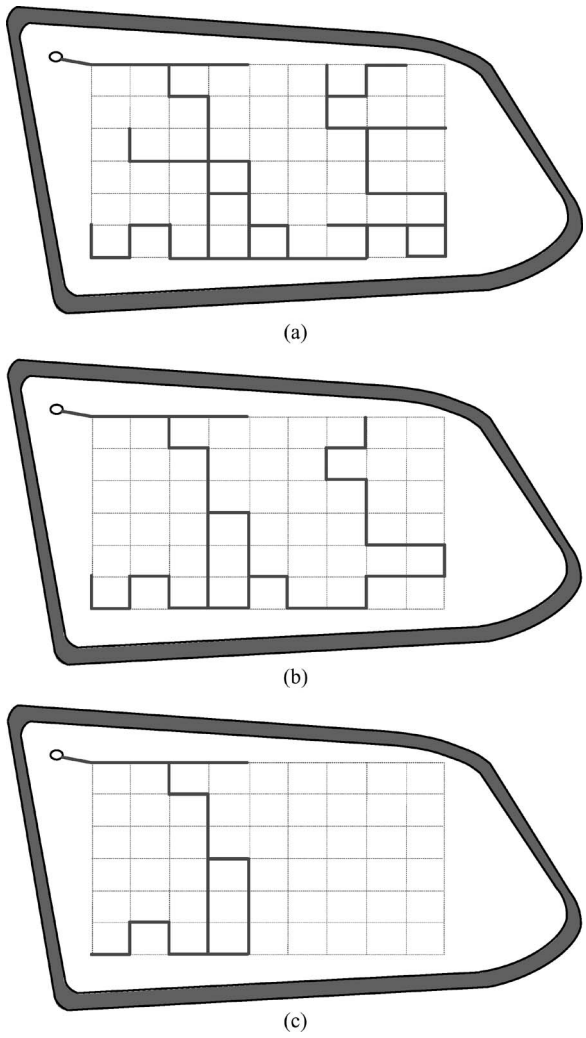

Fig. 8. Antenna shape after SSP. (a) First simplified on-glass antenna. (b) Second simplified on-glass antenna. (c) Third simplified on-glass.

diagram of TIP is similar to that of SSP, as shown in Fig. 10. The procedure starts by examining the current distributions on each strip. If the current on the strip is lower than a certain threshold value $(I_{\mathrm{threshold}} = -35$ dBA), then the width of the strip segment is reduced. The bore-sight gain of the design before and after the TIP is then compared to see the variation in antenna performance. This procedure is repeatedly applied until the gain variation is more than 3 dB. Fig. 11(a) is the design after TIP implementation and the antenna was divided into two regions ($I_{\mathrm{threshold}}$ of -35 dBA). In region A, the width of strip is 1 mm, whereas in region B, the width is reduced by 0.25 mm. Using the TIP, we can obtain high transparency of the antenna design by assigning a narrower width for certain strips. This is because reducing the width of strips with low current amplitude has relatively less effect on radiation efficiency and the antenna gain. Fig. 12(b) shows the bore-sight gain, depending on the widths of W_A and W_B in the individual regions. When W_A is 1 mm and W_B is 0.25 mm, the bore-sight gain of -9.03 dBi is almost the same as the design of $W_A = W_B =$ 1 mm. However, when both W_A and W_B are simulated at 0.25- and 0.1-mm widths, the average bore-sight gains are decreased to -11.52 and -42.82 dBi, respectively. Table II presents detailed comparisons of the average power loss, depending on

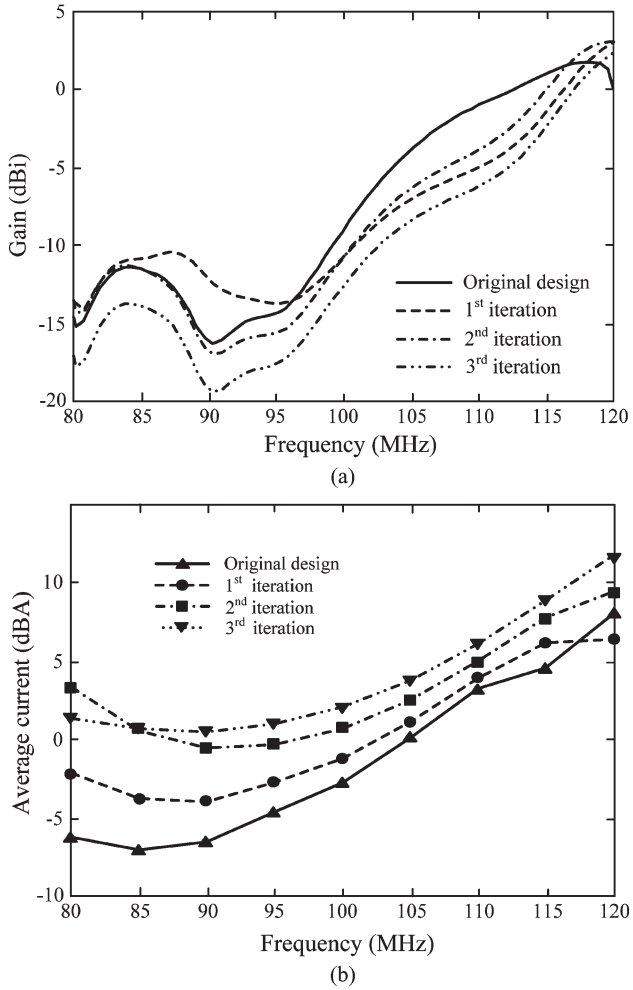

Fig. 9. Performance comparison of antenna using SSP. (a) Radiation gain of the bore sight. (b) Average current of the strip.

TABLE I
PERFORMANCE COMPARISON OF THE SIMPLIFIED ANTENNAS

Type	Optimized antenna	1st simplification	2nd simplification	3rd simplification
$I_{threshold}$	–55 dBA	–50 dBA	–45 dBA	–40 dBA
$Gain_{avg.}$	–7.47 dBi	–8.47 dBi	–8.67 dBi	–10.85 dBi
Space density	62/123 (50%)	51/123 (41%)	38/123 (31%)	21/123 (17%)

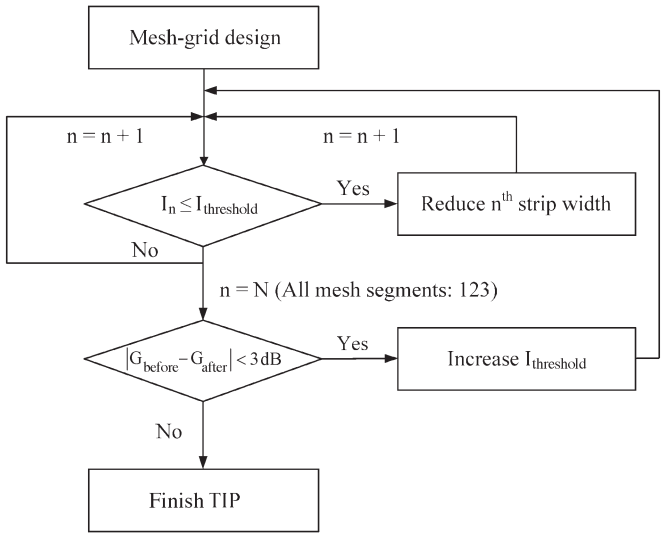

Fig. 10. Diagram of TIP.

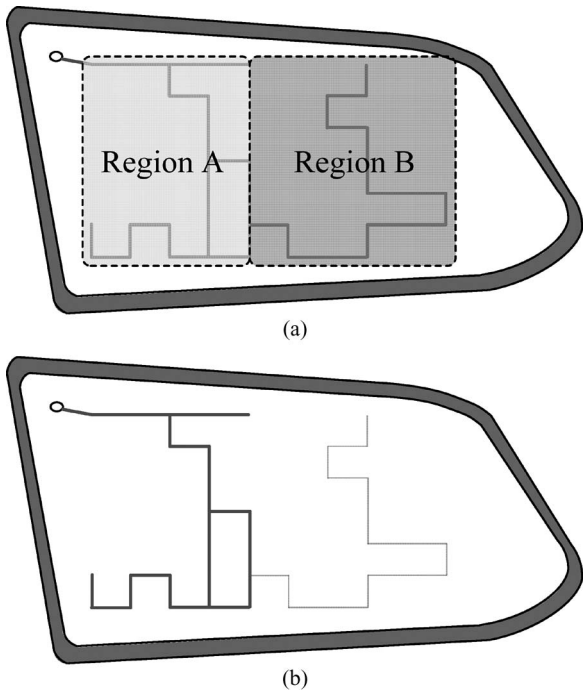

Fig. 11. Antenna shape after TIP. (a) Region division. (b) Antenna shape.

the strip width. When W_A is of 1-mm width and W_B is of 0.25-mm width, the average power loss of strips is 728 mW. These results are similar to the design that has a 1-mm width for both W_A and W_B. In the next chapter, we build and install the finalized on-glass antenna on a commercial RV and then measure antenna performances, such as the bore-sight gain and radiation pattern.

III. MEASUREMENT AND ANALYSIS OF THE ON-GLASS ANTENNA

A. Experimental Results

To verify the performance of the proposed antennas, we built three antennas. The first antenna (Ant. 1) is the design originally obtained by GA optimization only. The second antenna [Ant. 2, shown in Fig. 8(b)] is the design modified from Ant. 1 using second iterations of SSP, and the last one [Ant. 3, shown in Fig. 11(b)] is the finalized design after both SSP and TIP. All three antennas were built on the quarter glasses of the 2006 KIA Ground Carnival, and radiation characteristics were measured in a semianechoic chamber with dimensions of 30 m × 30 m [16]. The measured matching bandwidths ($|\Gamma| < 3$ dB) for Ant. 2 (17%) and Ant. 3 (22%) are very close to that of Ant. 1 (20%). Fig. 13 shows the measured bore-sight gain of (dash-dotted line) Ant. 1, (dashed line) Ant. 2, and (solid line) Ant. 3. Ant. 3 shows a bore-sight gain of −9.05 dBi in the entire FM radio band, which is very similar to that of Ant. 1 (−8.25 dBi) and Ant. 2 (−8.70 dBi), even though the

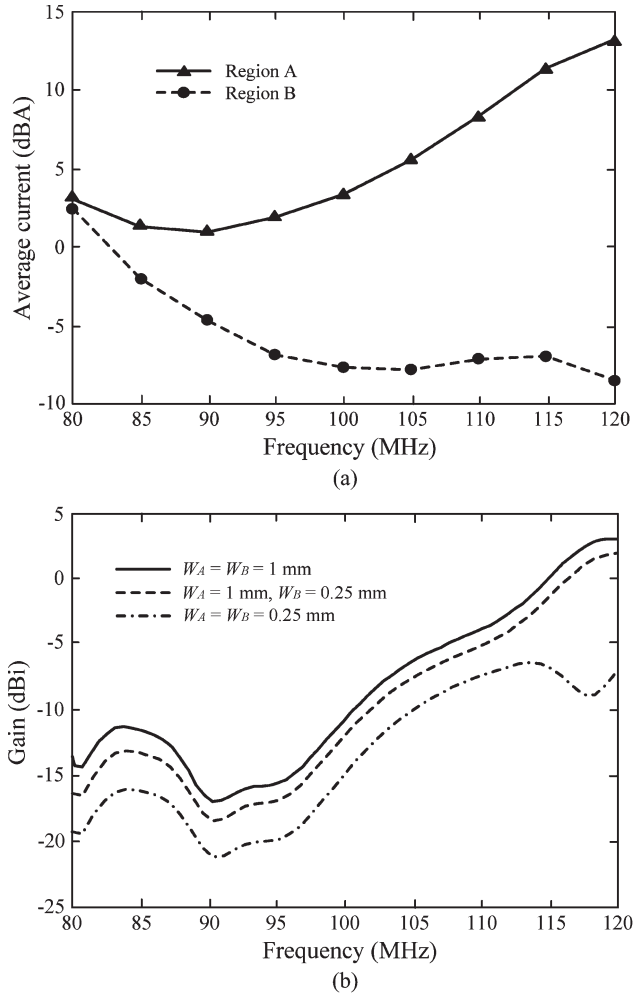

Fig. 12. Performance comparison of antenna using TIP. (a) Average current on the region. (b) Radiation gain along the bore-sight direction.

TABLE II
AVERAGE POWER LOSS BY THE STRIP WIDTH

Strip width	$W_A = W_B$ = 1 mm	W_A = 1mm, W_B = 0.25 mm	$W_A = W_B$ = 0.1 mm
Avg. power loss	714 mW	728 mW	858 mW

appearance of the design is improved from a manufacturing point of view.

To compare the performance such as reflection coefficient and bore-sight gain of the proposed antenna with that of the other antennas, we also measured a conventional $\lambda/4$ monopole (height $= 75$ cm, resonates at 100 MHz), a commercial on-glass antenna used for the 2006 KIA Ground Carnival, and a commercial microantenna (height $= 20$ cm). Ant. 3 shows the matching bandwidth of 22% ($|\Gamma| < 3$ dB, 108–130 MHz). The bandwidths for the conventional $\lambda/4$ monopole, commercial on-glass antenna, and microantenna are 26.2% (88.6–114.8 MHz), 9.6% (81.9–88.5 MHz), and 8.7% (94.5–103.2 MHz), respectively. Fig. 14 presents the measured bore-sight gain of (solid line) Ant. 3, (dotted line) conventional $\lambda/4$ monopole, (dash-dotted line) commercial on-glass antenna, and (dashed line) microantenna. Ant. 3 shows a superior bore-sight average gain with that of the commercial on-glass antenna (-12.49 dBi) and the microantenna (-18.88 dBi) and approaches the gain of the $\lambda/4$ monopole, of which the deviation is about 3 dB. We also examine the average gain over 360° azimuth and elevation gain, and results show -11.74, -6.01, -34.07, and -28.15 dBi for Ant. 3, the conventional $\lambda/4$ monopole, commercial on-glass antenna, and microantenna, respectively. Fig. 15 shows the measured radiation pattern of Ant. 3 in the azimuth plane. The maximum gain is shown in the bore sight of the antenna, and the gain variation in all azimuth directions is less than 20 dB. These results verify that the finalized on-glass antenna (Ant. 3) is suitable for FM radio reception with a visually improved appearance.

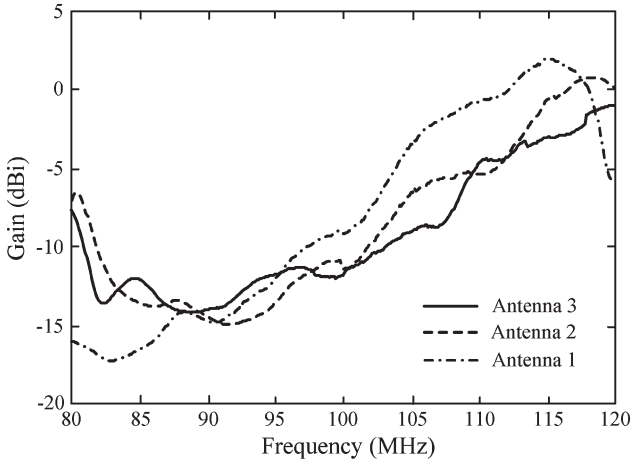

Fig. 13. Bore-sight gain of the finalized on-glass antenna.

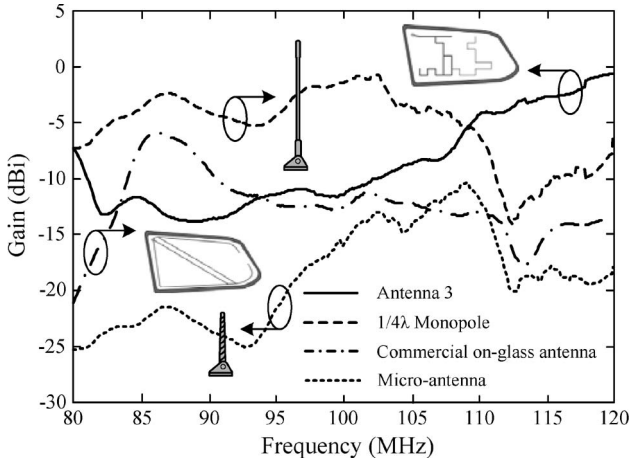

Fig. 14. Gain comparison of the various vehicle antennas.

B. Operating Principles

To efficiently receive the FM radio signals, the antennas provide high vertical gain, because the vertically polarized FM field is generally stronger than the other polarization due to field cancellation with the ground-reflected wave [17]–[20]. Fig. 16 shows the current distributions of the finalized on-glass antenna at 80, 100, and 120 MHz. We confirm that the left and right sides of the antenna induce a strong current in the same direction. These strongly induced vertical currents

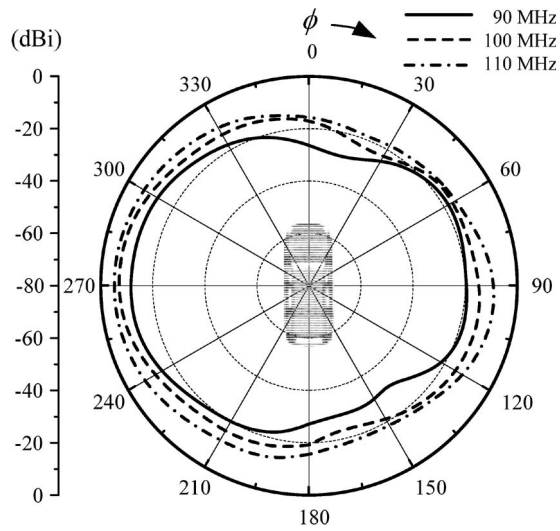

Fig. 15. Radiation patterns of the finalized antenna.

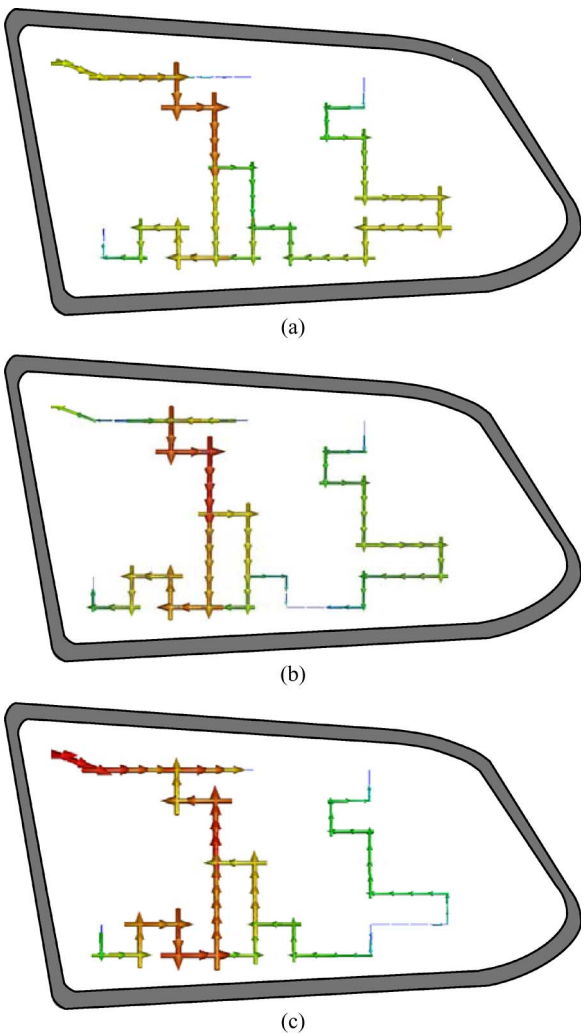

Fig. 16. Current distribution of the finalized antenna. (a) 80 MHz. (b) 100 MHz. (c) 120 MHz.

provide the high vertical gain of Ant. 3. The total electrical length of the antenna is three quarter-wavelengths ($\lambda = 3$ m at 100 MHz). One quarter-wavelength is for the left perpendicular strip, one quarter-wavelength is for the right perpendicular strip, and another one quarter-wavelength is for the middle horizontal strip. The antenna achieved a relatively good gain characteristic by optimally arranging the current distribution so that each quarter-wavelength of the current path works like an array element with the same phase. In addition, the second resonance of the finalized on-glass antenna reduces the high dielectric loss of the glass. The pole location where the direction of the current changes is placed at the middle horizontal strip; thus, the currents of the left and right perpendicular strip can have the same vertical direction.

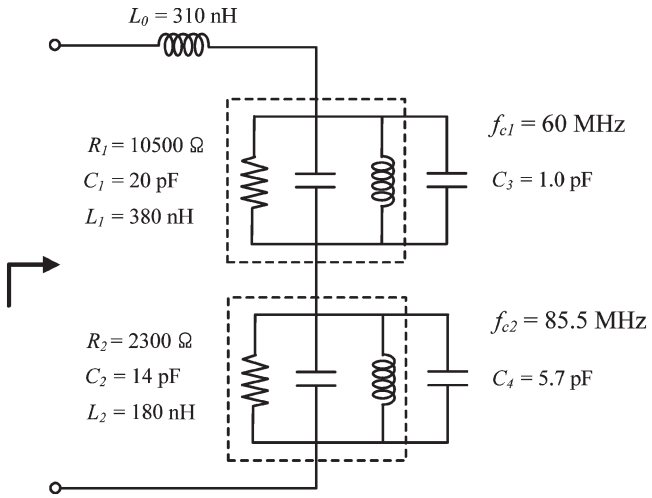

Fig. 17. Equivalent circuit model of the on-glass antenna.

To explain the frequency characteristics, we used a lumped element circuit for modeling the proposed antenna. The lumped element values are determined to model the impedance of the proposed antenna by a trial-and-error approach. Fig. 17 shows the resulting circuit model of the proposed antenna when the values for the lumped elements are the following: $L_0 = 310$ nH, $R_1 = 10\,500\ \Omega$, $L_1 = 380$ nH, $C_1 = 20$ pF, $R_2 = 2,300\ \Omega$, $L_2 = 180$ nH, and $C_2 = 14$ pF. The first parallel *RLC* circuit resonates at a frequency of 60 MHz, whereas the second parallel *RLC* circuit resonates at 85.5 MHz. Fig. 18 shows the input impedance using the equivalent circuit model in Fig. 17 and the EM simulation result. The impedance of the circuit model (solid line) is similar to the (dashed line) EM simulation result. Compared with the first resonance, the second resonance has lower Q values and, thus, shows a broad bandwidth characteristic.

IV. Conclusion

In this paper, we have proposed a mesh-grid on-glass antenna for receiving FM radio signals in RVs. For faster and more-accurate estimations of the proposed antenna performance, the strips have been modeled as a coated wire, and the vehicle structure was inserted in the EM simulation. We have optimized the antenna structure by using a GA in which we reduced the searching space and optimization time by using the CWF. We have also applied SSP and TIP so that the finalized on-glass antenna would minimize the obstruction of the passengers' view but produce similar results to the original design. The finalized

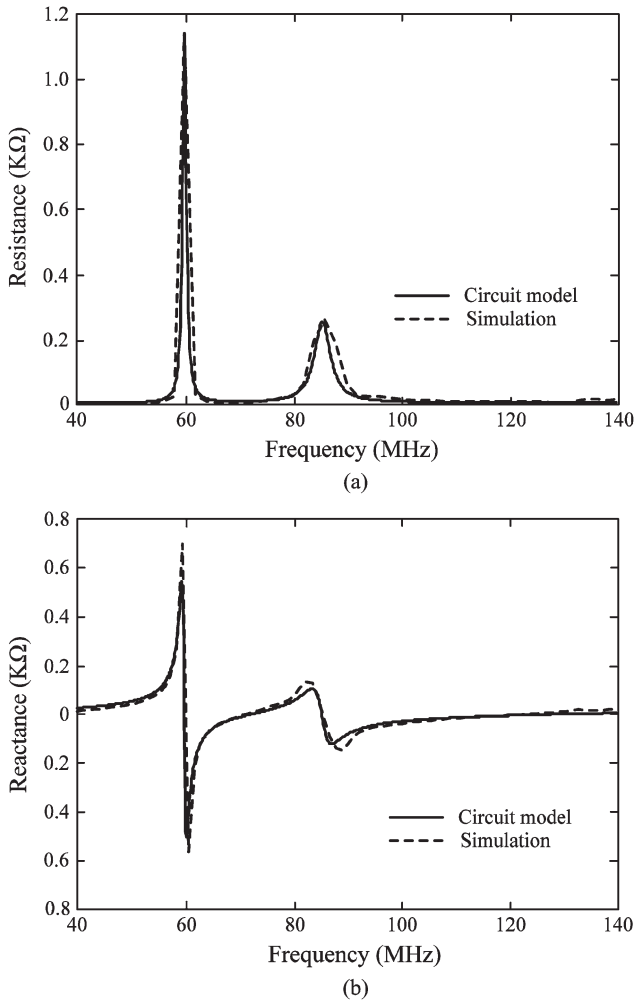

Fig. 18. Input impedance of the on-glass antenna. (a) Input resistance. (b) Input reactance.

antenna design has been built and measured in a semianechoic chamber. The average gain of the finalized antenna has been about −9.05 dBi, which is superior to that of a microantenna mounted on the roof of an RV by about 10 dB. Using the operating principle and current distributions of the mesh-grid on-glass antenna, we have confirmed that the proposed antenna had a high vertical gain and a broad bandwidth characteristic. This clearly shows that the proposed antenna is well suited for FM radio reception in a commercial RV.

REFERENCES

[1] S. Egashira, T. Tanaka, and A. Sakitani, "A design of AM/FM mobile telephone triband antenna," *IEEE Trans. Antennas Propag.*, vol. 42, no. 4, pp. 538–540, Apr. 1994.
[2] K. Yegin, "On-vehicle GPS antenna measurements," *IEEE Antennas Wireless Propag. Lett.*, vol. 6, pp. 488–491, Jun. 2007.
[3] L. Low, R. J. Langley, R. Breden, and P. Callaghan, "Hidden automotive antenna performance and simulation," *IEEE Trans. Antennas Propag.*, vol. 54, no. 12, pp. 3707–3712, Dec. 2006.
[4] R. Leelaratne and R. Langley, "Multiband PIFA vehicle telematics antennas," *IEEE Trans. Veh. Technol.*, vol. 54, no. 2, pp. 477–485, Mar. 2005.
[5] Y. Noh, Y. Kim, and H. Ling, "Broadband on-glass antenna with mesh-grid structure for automobiles," *Electron. Lett.*, vol. 41, no. 21, pp. 1148–1149, Oct. 2005.
[6] G. Clasen and R. J. Langley, "Meshed patch antenna integrated into car windscreen," *Electron. Lett.*, vol. 36, no. 9, pp. 781–782, Apr. 2000.
[7] J. C. Batchelor, R. J. Langley, and H. Endo, "On-glass mobile antenna performance modeling," in *Proc. Inst. Elect. Eng.—Microw. Antennas Propag.*, Aug. 2001, vol. 148, no. 4, pp. 233–238.
[8] R. Abou-Jaoude and E. K. Walton, "Numerical modeling of on-glass conformal automobile antennas," *IEEE Trans. Antennas Propag.*, vol. 46, no. 6, pp. 845–852, Jun. 1998.
[9] FEKO Comprehensive EM Solutions.
[10] W. P. King, "Wire and strip conductors over a dielectric-coated conducting or dielectric half-space," *IEEE Trans. Microw. Theory Tech.*, vol. 37, no. 4, pp. 754–760, Apr. 1989.
[11] R. W. P. King and T. T. Wu, "An analysis of coupled strip antenna and the strip transmission line," *Radio Sci.*, vol. 24, no. 1, pp. 27–34, Jan./Feb. 1989.
[12] J. Horn, N. Nafpliotis, and D. E. Goldberg, "A niched Pareto genetic algorithm for multiobjective optimization," in *Proc. IEEE Evol. Comput. Conf.*, 1994, vol. 1, pp. 82–87.
[13] Y. Rahmat-Samii and E. Michielssen, *Electromagnetic Optimization by Genetic Algorithms*. New York: Wiley, 1999.
[14] T. Hiroyasu, M. Miki, and S. Watanabe, "The new model of parallel genetic algorithm in multi-objective optimization problems—Divided range multi-objective genetic algorithm," in *Proc. Evol. Comput. Conf.*, 2000, vol. 1, pp. 333–340.
[15] Transmit antenna. [Online]. Available: http://www.ets-lindgren.com/manuals/3121C.pdf
[16] 2006 KIA Grand Carnival. [Online]. Available: http://www.kia.co.kr/
[17] M. Meeks, "VHF propagation over hilly, forested terrain," *IEEE Trans. Antennas Propag.*, vol. AP-31, no. 3, pp. 483–489, May 1983.
[18] C. A. Balanis, *Antenna Theory: Analysis and Design*, 3rd ed. New York: Wiley, 2005.
[19] K. Fujimoto and J. R. James, *Mobile Antenna Systems Handbook*, 2nd ed. Norwood, MA: Artech House, 2001.
[20] W. L. Stutzman and G. A. Thiele, *Antenna Theory and Design*, 2nd ed. New York: Wiley, 1997.

Seungbeom Ahn (S'10) was born in Gwangju, Korea, in 1978. He received the B.S. and M.S. degrees in electronic and electrical engineering in 2004 and 2006, respectively, from Hongik University, Seoul, Korea, where he is currently working toward the Ph.D. degree with the School of Electronic and Electrical Engineering.

His research interests are the study of on-glass antennas for vehicles and aircraft.

Hosung Choo (S'00–M'04) was born in Seoul, Korea, in 1972. He received the B.S. degree in radio science and engineering from Hanyang University, Seoul, in 1998 and the M.S. and Ph.D. degrees in electrical and computer engineering from the University of Texas, Austin, in 2000 and 2003, respectively.

From 1999 to 2003, he was a Research Assistant with the Department of Electrical and Computer Engineering, University of Texas. In September 2003, he joined the School of Electronic and Electrical Engineering, Hongik University, Seoul, where he is currently an Associate Professor. His research interests include the use of the optimization algorithm in developing antennas and microwave absorbers and the design of small antennas for wireless communications, reader and tag antennas for radio-frequency identification, and on-glass and conformal antennas for vehicles and aircrafts.